Absorption Approximation with Scattering Effect for Infrared Radiation

J. LI

Canadian Centre for Climate Modeling and Analysis, Atmospheric Environment Service, University of Victoria, Victoria, British Columbia, Canada

QIANG FU

Atmospheric Science Program, Department of Oceanography, Dalhousie University, Halifax, Nova Scotia, Canada

(Manuscript received 13 May 1999, in final form 30 September 1999)

ABSTRACT

A scheme that can handle cloud infrared scattering based on the absorption approximation is developed. In a two-stream mode, the new scheme produces more accurate results than those from the modified two-stream discrete ordinate method. For low and middle clouds, the two-stream version of the scheme produces a flux error less than 1 W m^{-2} and a heating rate error less than 0.5 K day^{-1}. With high clouds, the errors in calculated fluxes and heating rates are less than 1.4 W m^{-2} and 1.5 K day^{-1}, respectively. The four-stream version of the proposed scheme is slightly inferior to the four-stream discrete ordinate method. However, as opposed to the discrete ordinate technique, this scheme treats cloud-free layers the same as the absorption approximation. Therefore, numerically, it is much more efficient. Considering the radiative transfer module only, in a two-stream mode, the new scheme, which considers multiple scattering, uses only about 50% more CPU time than the absorption approximation method for a 100-layer column atmosphere with 20 cloudy layers.

1. Introduction

Generally, the radiative transfer process is very complicated. Fortunately, this process is dramatically simplified within earth's atmosphere by the following three factors: 1) for solar radiation, there is no source within the atmosphere; 2) the spectral overlap between the solar and infrared radiation is very small; and 3) for the infrared, radiative, scattering is weak. The third factor holds only for a clear sky, since the gaseous scattering (Rayleigh scattering) in the infrared is very weak and can be neglected. In most of the general circulation models (GCMs), the absorption (emissivity) approximation is used where scattering is neglected, though several recent studies have shown that infrared scattering by cloud droplets should not be neglected in climate models (Toon et al. 1989; Edwards and Slingo 1996; Fu et al. 1997; and others). Based on Fu et al. (1997), the outgoing infrared radiation can be overestimated by $\sim$4 W m^{-2} (assuming a cloud coverage of 0.6) due to the neglecting of infrared radiative scattering. Therefore, the infrared scattering may play an important role in the atmosphere. For example, neglecting infrared scattering increases the radiative cooling in the low clouds, which leads to more water vapor convergence into the cloud layer, thus generating more clouds.

Since scattering of infrared radiation does not exist in the cloud-free layers, it would be beneficial to find a way to account for scattering in cloud layers with the absorption approximation still applied to cloud-free layers. However, even if scattering occurs in a single atmospheric layer, the upward and downward intensities would be coupled together and the absorption approximation would no longer apply. A solution to this problem is the subject of this paper.

2. Theory and model development

The transfer equation for azimuthally averaged diffuse infrared intensity $I(\tau, \mu)$ is

$$\mu \frac{dI(\tau, \mu)}{d\tau} = I(\tau, \mu) - \frac{\tilde{\omega}}{2} \int_{-1}^{1} I(\tau, \mu') P(\mu, \mu')\, d\mu' - (1 - \tilde{\omega}) B(T), \quad (1)$$

where $\mu = \cos\theta$, θ is the local zenith angle, τ is the normal optical depth, $\tilde{\omega}$ is the single scattering albedo for cloud droplets, and $B(T)$ is blackbody emission at

Corresponding author address: Dr. Jiangnan Li, Canadian Centre for Climate Modeling and Analysis, Atmospheric Environment Service, P.O. Box 1700, University of Victoria, Victoria, BC V8P 2Y2, Canada.
E-mail: Jiangnan.Li@ec.gc.ca

temperature T. The integral in Eq. (1) is the source term representing the scattering effect. The azimuthal-independent phase function can be expanded in Legendre polynomials as

$$P(\mu, \mu') = \sum_{l=0}^{N} \tilde{\omega}_l P_l(\mu) P_l(\mu'), \tag{2}$$

where $P_l(\mu)$ is the l order Legendre polynomial. The moments $\tilde{\omega}_l$ can be determined from the orthogonal property of Legendre polynomials, with $\tilde{\omega}_0 = 1$ and $\tilde{\omega}_1 = 3g$, where g is asymmetry factor.

For a nonisothermal layer, the optical depth dependence of the Planck function is needed. In most current GCMs, a constant Planck function determined by the temperature at the center of the layer is used. Hereafter, following Fu and Liou (1993) and Fu et al. (1997), an exponential optical depth dependence for the Planck function is assumed such that

$$B[T(\tau)] = \alpha e^{\beta\tau}, \tag{3}$$

where $\alpha = B_0$ and $\beta = (1/\tau_l) \ln(B_1/B_0)$, with B_0 and B_1 being the Planck functions for the temperature at the top and the bottom of the layer, respectively, and τ_l is the optical depth of the layer.

For the infrared, absorption is strong and scattering is weak. Usually, the infrared scattering process is simplified and the radiative transfer equation [Eq. (1)] is

$$\mu \frac{dI(\tau, \mu)}{d\tau} = (1 - \tilde{\omega}) I(\tau, \mu) - (1 - \tilde{\omega}) B(T) \tag{4}$$

and this is referred to as absorption approximation. The solution of Eq. (4) is

$$I(0, \mu) = I(\tau_l, \mu) e^{-\epsilon\tau_l/\mu} + \frac{\epsilon}{\mu\beta - \epsilon}(B_1 e^{-\epsilon\tau_l/\mu} - B_0), \tag{5a}$$

$$I(\tau_l, -\mu) = I(0, -\mu) e^{-\epsilon\tau_l/\mu} + \frac{\epsilon}{\mu\beta + \epsilon}(B_1 - B_0 e^{-\epsilon\tau_l/\mu}), \tag{5b}$$

where $\epsilon = 1 - \tilde{\omega}$ is the coalbedo.

Equations (5a) and (5b) give the upward and downward intensities. The corresponding upward and downward fluxes can be obtained as

$$F^+(0) = 2\pi \int_0^1 I(0, \mu)\mu \, d\mu, \tag{6a}$$

$$F^-(\tau_l) = 2\pi \int_0^{-1} I(\tau_l, \mu)\mu \, d\mu = 2\pi \int_0^1 I(\tau_l, -\mu)\mu \, d\mu. \tag{6b}$$

The angular integrations can be evaluated by the Gaussian quadrature method. There are many choices for Gaussian quadratures. By directly using a Gaussian quadrature with moment equal to zero, we obtain the μ weighted mean (μWM) results:

$$F^+(0) = 2\pi \int_0^1 I(0, \mu)\mu \, d\mu = 2\pi \sum_{i=1}^{n} w_i \mu_i I(0, \mu_2), \tag{7a}$$

$$F^-(\tau_l) = 2\pi \int_0^1 I(\tau_l, -\mu)\mu \, d\mu = 2\pi \sum_{i=1}^{n} w_i \mu_i I(\tau_l, -\mu_i). \tag{7b}$$

The weight w_i and abscissa μ_i with node $n = 1, 2, 3$ for μWM are given in Li (2000). For $n = 1$, we have $\mu_1 = ½$, which is the so-called hemispheric mean. Fu et al. (1997) and Li (2000) show that the hemispheric mean generally does not provide accurate results. Li (2000) also shows that the other Gaussian quadrature with different moment powers can also be used to evaluate the infrared radiative fluxes, which generally gives

$$F^+(0) = 2\pi \int_0^1 I(0, \mu)\mu \, d\mu = 2\pi \sum_{i=1}^{n} w_i I(0, \mu_i), \tag{8a}$$

$$F^-(\tau_l) = 2\pi \int_0^1 I(\tau_l, -\mu)\mu \, d\mu = 2\pi \sum_{i=1}^{n} w_i I(\tau_l, -\mu_i). \tag{8b}$$

The weight w_i and abscissa μ_i with node $n = 1, 2, 3$ for different moment powers are shown in Li (2000). For a moment power approaching infinity, the Gaussian quadrature of node $n = 1$ produces a $\mu_1 = 1/e^{1/2} = 1/1.648\,721\,3$, which is very close to the diffuse factor $\mu_1 = 1/1.66$ for flux transmittance. Therefore, we will use the Gaussian quadrature with infinite moment power to evaluate the flux integration for node $n = 1$. This is called the two-stream absorption approximation (2AA), since the fluxes are determined by two angles of $\pm\mu_1$. We would like to point out that the question here is not to evaluate an integration for the flux transmittance but to evaluate an integration for the intensity, which is more complicated than the flux transmittance. We simply cannot use the diffuse factor method, which is derived specially for the flux transmittance. Therefore, a Gaussian quadrature with a solid mathematical foundation has to be used. For $n = 2$ [four-stream absorption approximation (4AA)], we use the μWM of Eq. (7) to calculate the flux because μWM produces a slightly better result for the high cloud case compared to that of Eq. (8). The formulas of Gaussian quadrature used in the following

calculations for the two-stream (node $n = 1$) and four-stream (node $n = 2$) are shown in Table 1. The general discussion for Gaussian quadrature in evaluation of flux is shown in Li (2000).

In Eq. (5), the upward and downward intensities are decoupled. This makes the calculation of intensity extremely simple. The upward intensity at the top of a layer is determined by the upward intensity incident on the bottom of the layer and the thermal emission inside the layer, and similarly for the downward intensity. The calculations of the upward and downward intensities are totally independent. Because of this simplicity, the absorption approximation is widely used in climate models.

For clear sky, Eq. (5) is accurate because the single-scattering albedo $\tilde{\omega} = 0$ (i.e., no scattering), but for cloudy sky, scattering is no longer negligible. If scattering is considered, the upward and downward intensities will be coupled due to reflectance incurred by scattering cloud droplets. The upward and downward intensities have to be considered at the same time for all the layers in a column. Usually, a matrix inverse method is used for solving the coupled upward and downward infrared radiation (Toon et al. 1989; Fu et al. 1997; etc.).

In a matrix inverse method, a higher stream discrete ordinate scheme is much more expensive compared to that of the two-stream discrete ordinate scheme. However, the two-stream discrete ordinate scheme often produces inaccurate results in some cases. Toon et al. (1989) and Fu et al. (1997) used a source function technique to solve this problem. Since the cloud scattering effect in the infrared is weak, the results of intensity obtained by the two-stream discrete ordinate scheme can be used for the source term in Eq. (1). When the source function is known, the radiative transfer equation becomes decoupled for the upward and downward intensities. Then, the solution for intensity can be easily found and the flux can be obtained using Eqs. (7) and (8). Because the calculation of the decoupled intensity is simple, a higher stream scheme can be used to calculate the flux. It is shown that source function technique can provide more accurate results compared to the two-stream discrete ordinate scheme, especially for high clouds. We would like to point out that the source function technique is intrinsically a perturbation method, which uses the results of a lower-order equation and substitutes them in the less important part of the higher-order equation to simplify the problem (Li et al. 1994, 1995).

Although the source function technique can provide accurate results and save computing time compared to a higher-stream discrete ordinate scheme, the inverse matrix for the two-stream calculation is still needed. Generally, the matrix inversion method is much more expensive compared to the absorption approximation because the layers with or without scattering are treated equally in the matrix inversion process. Besides, it is not straightforward to deal with fractional clouds in a matrix inverse method. Our goal is to avoid the scattering calculation for cloud-free layers. The perturbation has to be based on the absorption approximation to obtain the intensity needed for the source term. Therefore, the radiative transfer equation becomes

$$\mu \frac{dI(\tau, \mu)}{d\tau} = I(\tau, \mu) - \frac{\tilde{\omega}}{2} \int_{-1}^{1} I^0(\tau, \mu') P(\mu, \mu')\, d\mu' - \epsilon B(T) \tag{9}$$

where I^0 is obtained from Eq. (5). We denote the scattering term in Eq. (9) as $M(\tau, \mu)$. The term $I^0(\tau, \mu)$ can be discrete based on how many streams are considered; thus,

$$\begin{aligned} M(\tau, \mu) &= \frac{\tilde{\omega}}{2} \int_{-1}^{1} I^0(\tau, \mu') P(\mu, \mu')\, d\mu' \\ &= \frac{\tilde{\omega}}{2} \sum_{l=0}^{N} P_l(\mu) \sum_{\substack{j=-n \\ j\neq 0}}^{n} I^0(\tau, \mu_j) P_j(\mu_j) w_j \\ &= \frac{\tilde{\omega}}{2} \sum_{\substack{j=-n \\ j\neq 0}}^{n} \psi(\mu, \mu_j) I^0(\tau, \mu_j) w_j, \end{aligned} \tag{10}$$

with

$$\psi(\mu, \mu_j) = 1 + \tilde{\omega}_1 P_1(\mu) P_1(\mu_j) + \tilde{\omega}_2 P_2(\mu) P_2(\mu_j) + \cdots + \tilde{\omega}_N P_N(\mu) P_N(\mu_j). \tag{11}$$

Here $\psi(\mu, \mu_j)$ represents the fractional intensity of $I^0(\tau, \mu_j)$ being scattered into the direction of μ. In the discrete-ordinate method, the number of expansion terms, N, is related to the stream number, n, by $N = 2n - 1$. However, since $I(\tau, \mu)$ and $I^0(\tau, \mu_j)$ are not directly related, there is no restriction on the expansion term in Eq. (11). For simplicity, only the first two terms of Eq. (11) are kept in the calculations, $\psi(\mu, \mu_j) = 1 + 3g\mu\mu_j$. In the calculation of I^0, scattering is neglected, so there is not an exact phase function relation between I and I^0. To keep a higher-order expansion may not bring better results. Besides, in the parameterization of cloud optical properties, only the first moment (i.e., the asymmetry factor) is usually considered. Based on the first-order expansion of the phase function, optical property adjustments follow Joseph et al. (1976). Note that the effective cloud optical depth $(1 - \tilde{\omega})\tau$ in absorption approximation does not change under such adjustment.

In Eq. (9), integration of the scattering source term is known, so upward and downward intensities are decoupled. The solution is

TABLE 1. Abscissa and weight factors for Gaussian integration for two-stream and four-stream.

	Two stream ($n = 1$) $\int_0^1 f(\mu)\mu\, d\mu \simeq \sum_{i=1}^n w_i f(\mu_i)$		Four stream ($n = 2$) $\int_0^1 f(\mu)\mu\, d\mu \simeq \sum_{i=1}^n w_i \mu_i f(\mu_i)$	
n	$1/\mu_i$	w_i	$1/\mu_i$	w_i
1	1.6487213	1.0000000		
2			4.7320500	0.5000000
			1.2679492	0.5000000

$$I(0, \mu) = I(\tau_l, \mu)e^{-\tau_l/\mu} + S^+(\tau_l, \mu) - \frac{\epsilon}{-\beta\mu + 1}(B_1 e^{-\tau_l/\mu} - B_0), \quad (12a)$$

$$I(\tau_l, -\mu) = I(0, -\mu)e^{-\tau_l/\mu} + S^-(\tau_l, -\mu) + \frac{\epsilon}{\beta\mu + 1}(B_1 - B_0 e^{-\tau_l/\mu}). \quad (12b)$$

The contribution to intensity from the scattering effect is

$$\begin{aligned} S^+(\tau_l, \mu) &= \frac{1}{\mu}\int_0^{\tau_l} M(\tau, \mu)e^{-\tau/\mu}\, d\tau \\ &= \frac{\tilde{\omega}}{2}\left\{\frac{\psi(\mu, -\mu_1)}{\epsilon\mu/\mu_1 + 1}(1 - e^{-\epsilon\tau_l/\mu_1}e^{-\tau_l/\mu_1})[I^0(0, -\mu_1) - \eta(\mu_1)B_0]\right. \\ &\quad + \frac{\psi(\mu, \mu_1)}{\epsilon\mu/\mu_1 - 1}(e^{-\tau_l/\mu} - e^{-\epsilon\tau_l/\mu_1})[I^0(\tau_l, \mu_1) - \eta(-\mu_1)B_1] \\ &\quad \left. + \frac{1}{\beta\mu - 1}[\eta(\mu_1)\psi(\mu, -\mu_1) + \eta(-\mu_1)\psi(\mu, \mu_1)](B_1 e^{-\tau_l/\mu} - B_0)\right\} w_1 + \underline{(\mu_1 \to \mu_2, w_1 \to w_2)} \\ &\quad + \underline{(\mu_1 \to \mu_3, w_1 \to w_3)} + \cdots, \end{aligned} \quad (13)$$

where $\eta(\mu) = \epsilon/(\beta\mu + \epsilon)$. Note that $(\underline{\mu_1 \to \mu_2, w_1 \to w_2})$ means the same formula as the first part but with replacement of $\mu_1 \to \mu_2$ and $w_1 \to w_2$. This applies to the two-node Gaussian quadrature (four stream) case. The same is for $(\underline{\mu_1 \to \mu_3, w_1 \to w_3})$, which applies to the three-node Gaussian quadrature (six stream). In principle, Eq. (13) can be applied to any node Gaussian quadrature.

Since the physical process is the same for the upward and downward intensities, the expression $S^-(\tau_l, -\mu)$ for the downward intensity should be the same as $S^+(\tau_l, \mu)$ except that the physical quantities related to "up" and "down" should exchange as

$$I^0(0, \mu_i) \leftrightarrow I^0(\tau_l, -\mu_i), \qquad B_0 \leftrightarrow B_1, \qquad \mu \leftrightarrow -\mu, \qquad \mu_i \leftrightarrow -\mu_i.$$

Note that the last two exchanges should not be applied to $e^{-\tau_l/\mu}$ and $e^{-\epsilon\tau_l/\mu_i}$, since they represent the internal intensity decay from the boundary. The exchanges listed above for $S^+(\tau_l, \mu)$ and $S^-(\tau_l, \mu)$ are also true for Eq. (5), Eq. (12), and other similar equations regarding upward and downward intensities.

In clear sky, $\tilde{\omega} = 0$, $S^+(\tau_l, \mu)$ and $S^-(\tau_l, \mu)$ are equal to zero, and Eq. (12) reduces to Eq. (5).

For 2AA, μ will be specified to $\mu_1 = 1/1.648\,721\,3$ in Eq. (13) with weight $w_1 = 1$. For 4AA, μ will be specified to μ_1 and μ_2 in Eq. (13) with weights w_1 and w_2 given in Table 1 for μWM. In Eq. (13), the physics of the three terms for weight w_1 is very clear. They are the effect of the backward scattering, forward scattering, and internal anisotropic scattering, respectively. The limiting cases of optical depth approaching to zero and infinity are always a good test for the validity of a theory. We have

$$\lim_{\tau_l \to 0} S^+(\tau_l, \mu) = 0,$$

and there is no contribution from the scattering effect; in

$$\lim_{\tau_l \to \infty} S^+(\tau_l, \mu) = \frac{\tilde{\omega}}{2}\left\{\frac{\psi(\mu, -\mu_1)}{\epsilon\mu/\mu_1 + 1}[I^0(0, -\mu_1) - B_0] - [\psi(\mu, -\mu_1) + \psi(\mu, \mu_1)]B_0\right\},$$

the contributions from the forward scattering disappear. This is what is expected, since forward intensity from the lower boundary decays to zero for infinite optical depth.

In summary, the calculation process is based on two steps. First, we use the absorption approximation to obtain the intensity solutions at each model level. These are not the true values but should be close to the accurate

values, since the cloud infrared scattering is weak. Second, we use the obtained intensity to recalculate the radiative intensity again, with the scattering effect included.

As mentioned before, most GCMs use a constant Planck function for each model layer. In this case, $\beta = 0$ and $B_0 = B_1 = B_c$, where B_c is the Planck function for temperature at the center of the layer. Equations (12) and (13) will be simplified under this condition.

3. Results

In the previous section, the multiple-stream ($2n$AA) absorption approximation and a scheme of $2n$-stream absorption approximation, including scattering effects ($2n$AAS), were presented. In this section, their accuracy will be examined. We will focus on the two-stream and four-stream cases and compare the results with the corresponding results of the modified two-stream approximation (D2S) and four-stream approximation (D4S) shown in Fu et al. (1997). Benchmark values are obtained from the δ-128-stream discrete ordinate model (D128) (Stamnes et al. 1988).

In the clear sky, the results of the radiative flux and heating rate for 2AA and 2AAS are the same, which are very close to the results of D2S. The differences in fluxes are less than 0.1%. The same is true for 4AA, 4AAS, and D4S. Since the clear sky case has been shown in Fu et al. (1997), we will discuss only the cloudy sky cases in this work. The radiation model is the same as that of Fu et al. (1997), which is based on the correlated *k*-distribution method for gaseous transmission (Fu and Liou 1992). Two atmospheric profiles are used: the midlatitude summer (MLS) and the subarctic winter (SAW). Here we use the same cloud cases as in Fu et al. (1997). A low cloud is positioned from 1.0 to 2.0 km in MLS and from 0.5 to 1.5 km in SAW, with a liquid water content (LWC) of 0.22 g m^{-3} and an effective radius (r_e) of 5.98 μm. A middle cloud is positioned from 4.0 to 5.0 km in MLS and from 2.0 to 3.0 km in SAW, with LWC = 0.28 g m^{-3} and $r_e = 6.2$ μm. A high cloud is positioned from 10 to 12 km in MLS and from 6 to 8 km in SAW, with an ice water content (IWC) of 0.0048 g m^{-3} and a mean effective size (D_e) of 41.5 μm.

Figure 1 shows errors in the heating rate for the low cloud in MLS (upper panels) and SAW (lower panels). The left column shows the results for 2AA and 4AA. The difference between 2AA and 4AA is very small. The optical depth for the low cloud is large, and the multiple-scattering process makes the radiation isotropic inside the cloud layer. Therefore, the increase in stream number does not help to increase the accuracy. The same is true for the flux shown in Tables 2 and 3. The errors in heating rate and flux are large for 2AA and 4AA. The error in heating rate is up to almost 3 K day^{-1}, and the error in upward flux at the top of the atmosphere is up to 5 W m^{-2} in MLS.

These errors are reduced much for D2S and 2AAS, as shown in the middle column. The error in heating rate for MLS is less than 1 K day^{-1} for D2S and less than 0.3 K day^{-1} for 2AAS. Also, 2AAS always produces better results in flux compared with D2S, and the errors for upward flux at the top of the atmosphere are always less than 1 W m^{-2} for 2AAS.

The error in heating rate can be reduced further by using a four-stream scheme. Both D4S and 4AAS produce errors in heating rate less than 0.25 K day^{-1} for MLS (right column in Fig. 1). For SAW, 4AAS is slightly inferior to D4S in heating rate. Also, the error in the upward flux at the top of the atmosphere for 4AAS is slightly greater than that of D4S for MLS and SAW.

Figure 2 shows the results for the middle cloud. The errors in heating rate for 2AA and 4AA are up to 4 K day^{-1} in MLS. Such errors are reduced to 1.3 K day^{-1} for D2S and to 0.35 K day^{-1} for 2AAS. The same goes for flux (Tables 2 and 3); 2AAS always produces better results compared with D2S. The right column of Fig. 2 shows the results of D4S and 4AAS. As the low cloud case, 4AAS is slightly inferior to D4S.

Figure 3 shows the results for the high cloud. It is found that 4AA produces much better results in heating rate compared with 2AA. This clearly demonstrates that the error for a high cloud in 2AA is mostly caused by improper handling of the highly anisotropic radiation inside the high clouds. For high clouds, the optical depth is usually thin, and outgoing photons undergo only a few scattering events. Thus, the results are strongly dependent upon the single scattering direction, and intensity is therefore highly anisotropic. The two-stream approximation in which only two specified angles are considered cannot handle such anisotropic radiation. Therefore, a higher-stream approximation has to be used. This is confirmed in the middle column for D2S and 2AAS. The results become only slightly better by including the scattering effect. The results of D4S and 4AAS are the best, since both the scattering effect and anisotropic intensity are well handled.

Figure 4 shows the results of the low, middle, and high clouds together. The situation in heating rate for each cloud is very similar to that of the individual cloud cases shown above. The 4AA can dramatically improve the results for the high cloud; 2AAS is always better than D2S; 4AAS is slightly inferior to D4S. The errors in flux are also shown in Tables 2 and 3. The best results are 2AAS and D4S; 4AAS is slightly inferior to 2AAS and D4S but slightly better than D2S. The worst results are 2AA and 4AA.

The above results are based on very high vertical resolution with a layer thickness of 0.25 km. In GCMs, the model vertical resolution is usually much coarser. Therefore, we would like to investigate the corresponding results with a lower model vertical resolution. We consider an atmospheric profile of MLS with the vertical resolution of layer thickness 1 km. Table 4 shows the errors in flux for the low cloud, middle cloud, high

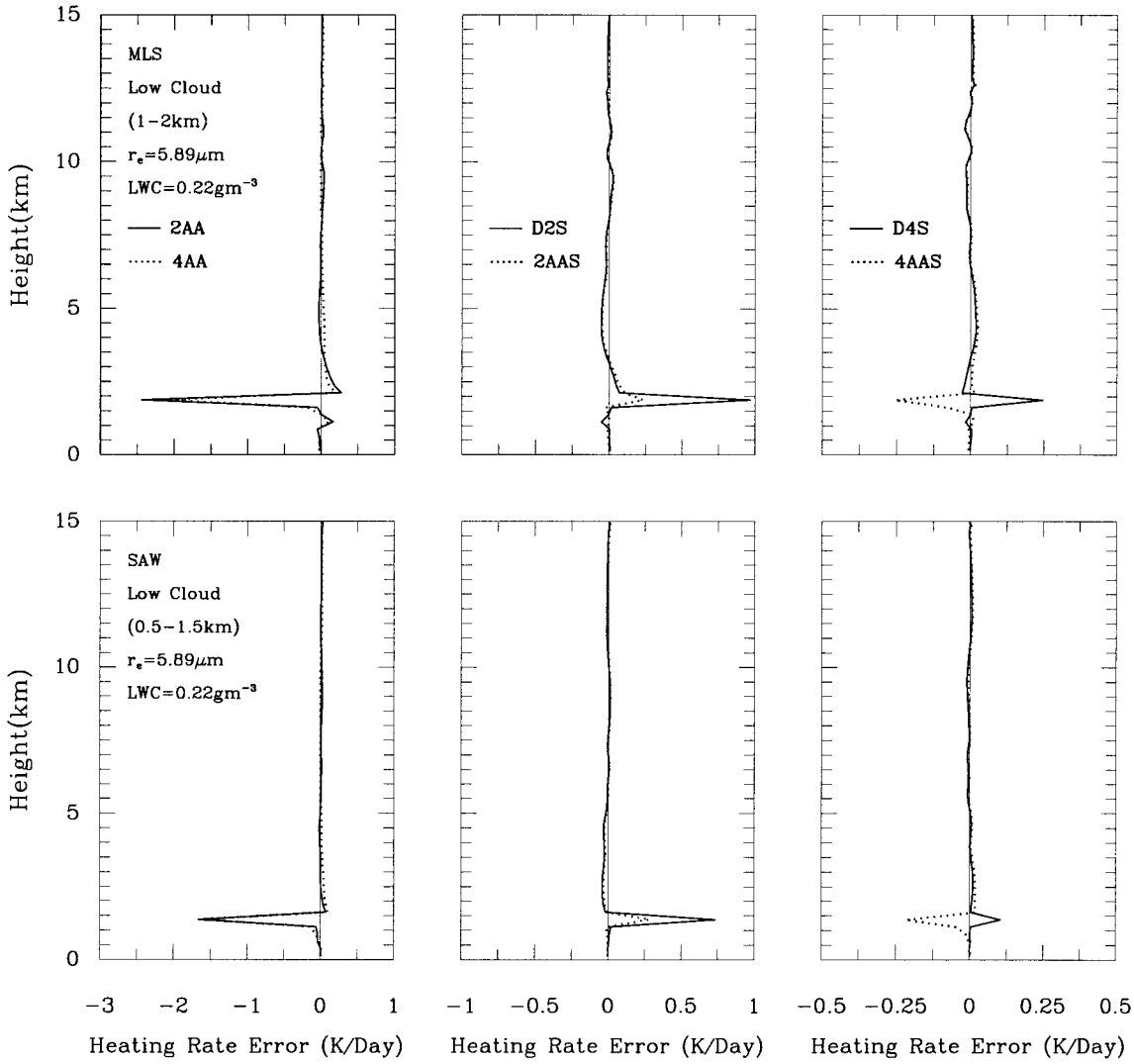

FIG. 1. The absolute errors of 2AA, 4AA; D2S, 2AAS; and D4S, 4AAS for MLS (upper panels) and for SAW (lower panels). The model with vertical resolution of layer thickness 0.25 km. The low cloud (in position from 1.0 to 2.0 km in MLS and from 0.5 to 1.5 km in SAW) is contained.

TABLE 2. Comparison of various radiative schemes for infrared fluxes (W m^{-2}) at the top and surface using MLS. The numbers in the parentheses give differences (W m^{-2}) between approximate method and the δ-128-stream. The model with vertical resolution of layer thickness 0.25 km.

Cloud conditions	D128S	2AA	2AAS	D2S	4AA	4AAS	D4S
				$F^{\uparrow}$ (TOA)			
Low cloud	266.0	271.3 (5.3)	265.7 (−0.3)	264.1 (−1.9)	270.9 (4.9)	267.0 (1.0)	265.8 (−0.2)
Middle cloud	229.6	236.1 (6.5)	229.4 (−0.2)	227.8 (−1.8)	235.6 (6.0)	230.7 (1.1)	229.4 (−0.2)
High cloud	215.6	222.0 (6.4)	215.2 (−0.3)	214.1 (−1.5)	222.4 (6.8)	215.2 (−0.4)	214.9 (−0.7)
Low, middle, and high clouds	188.0	196.4 (8.4)	187.7 (−0.3)	186.2 (−1.8)	196.1 (8.1)	188.4 (0.4)	187.6 (−0.4)
				$F^{\downarrow}$ (SFC)			
Low cloud	412.1	411.5 (−0.6)	412.0 (−0.1)	412.2 (0.1)	411.6 (−0.5)	411.9 (−0.2)	412.0 (−0.1)
Middle cloud	393.6	392.3 (−1.3)	393.7 (0.1)	394.2 (0.6)	392.6 (−1.0)	393.5 (−0.1)	393.8 (0.2)
High cloud	355.1	355.3 (0.2)	356.2 (0.9)	356.6 (1.5)	355.0 (−0.1)	355.7 (0.6)	355.6 (0.5)
Low, middle, and high clouds	412.1	411.5 (−0.6)	412.0 (−0.1)	412.2 (0.1)	411.6 (−0.5)	411.9 (−0.2)	412.0 (−0.1)

TABLE 3. Same as in Table 2 except for SAW.

Cloud conditions	D128S	2AA	2AAS	D2S	4AA	4AAS	D4S
				$F^{\uparrow}$ (TOA)			
Low cloud	196.9	201.4 (4.5)	196.6 (−0.3)	195.4 (−1.5)	201.0 (4.1)	197.4 (0.5)	196.6 (−0.3)
Middle cloud	188.2	193.0 (4.8)	187.8 (−0.4)	186.7 (−1.5)	192.6 (4.4)	188.8 (0.6)	187.9 (−0.3)
High cloud	169.5	174.1 (4.6)	169.3 (−0.2)	168.7 (−0.8)	173.8 (4.3)	169.1 (−0.4)	168.8 (−0.7)
Low, middle, and high clouds	163.9	169.9 (6.0)	163.4 (−0.5)	162.3 (−1.6)	169.6 (5.7)	164.0 (0.1)	163.4 (−0.5)
				$F^{\downarrow}$ (SFC)			
Low cloud	249.1	249.2 (0.1)	249.0 (−0.1)	249.0 (−0.1)	249.2 (0.1)	249.1 (0.0)	249.0 (−0.1)
Middle cloud	245.3	245.1 (−0.2)	245.3 (0.0)	245.3 (0.0)	245.0 (−0.3)	245.2 (−0.1)	245.2 (−0.1)
High cloud	188.7	188.2 (−0.5)	189.7 (1.0)	190.1 (1.4)	187.3 (−1.4)	189.0 (0.3)	188.9 (0.2)
Low, middle, and high clouds	249.1	249.2 (0.1)	249.0 (−0.1)	249.0 (−0.1)	249.2 (0.1)	249.1 (0.0)	249.0 (−0.1)

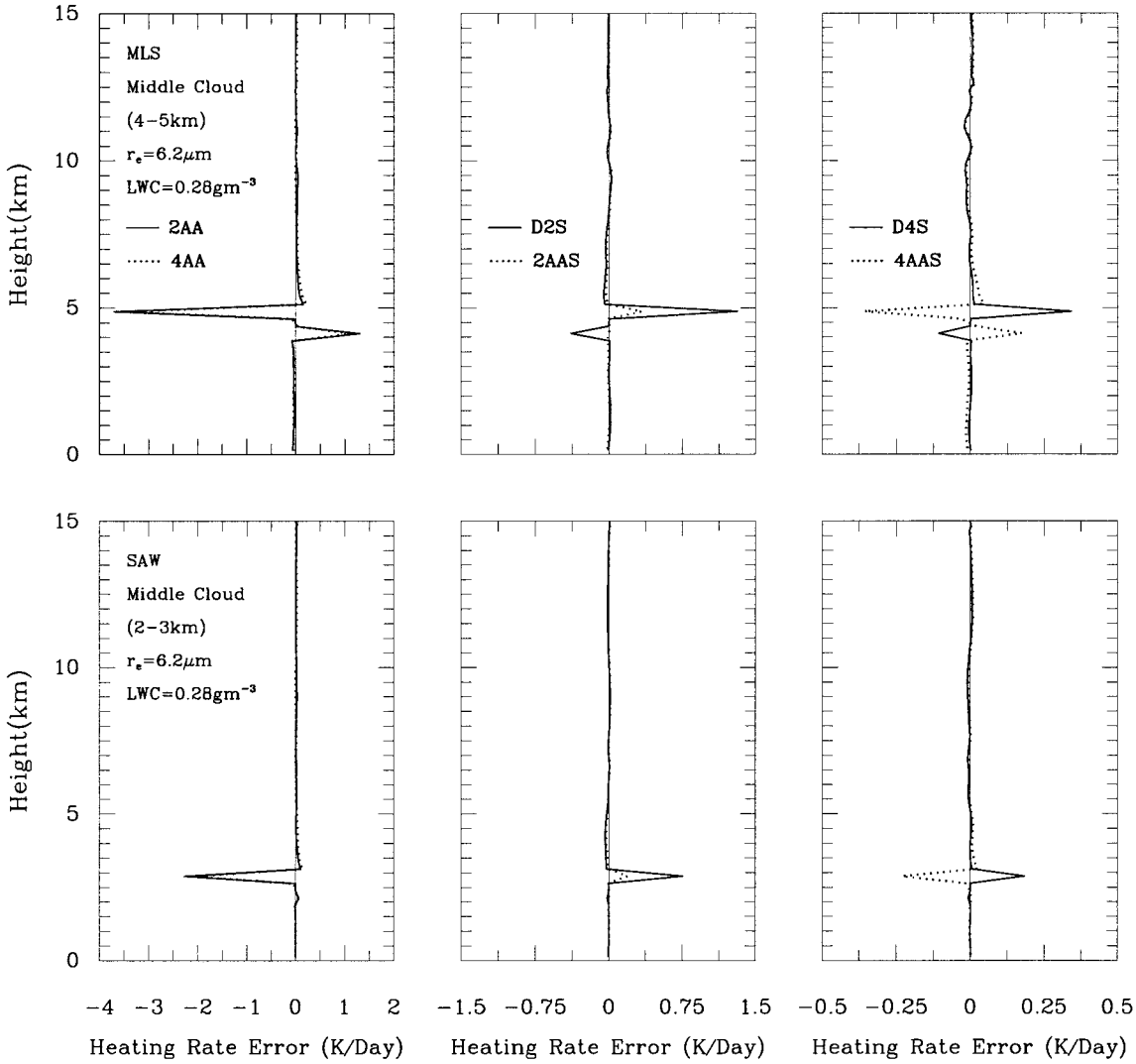

FIG. 2. As in Fig. 1 except for the sky containing the middle cloud (in position from 4.0 to 5.0 km in MLS and from 2.0 to 3.0 km in SAW).

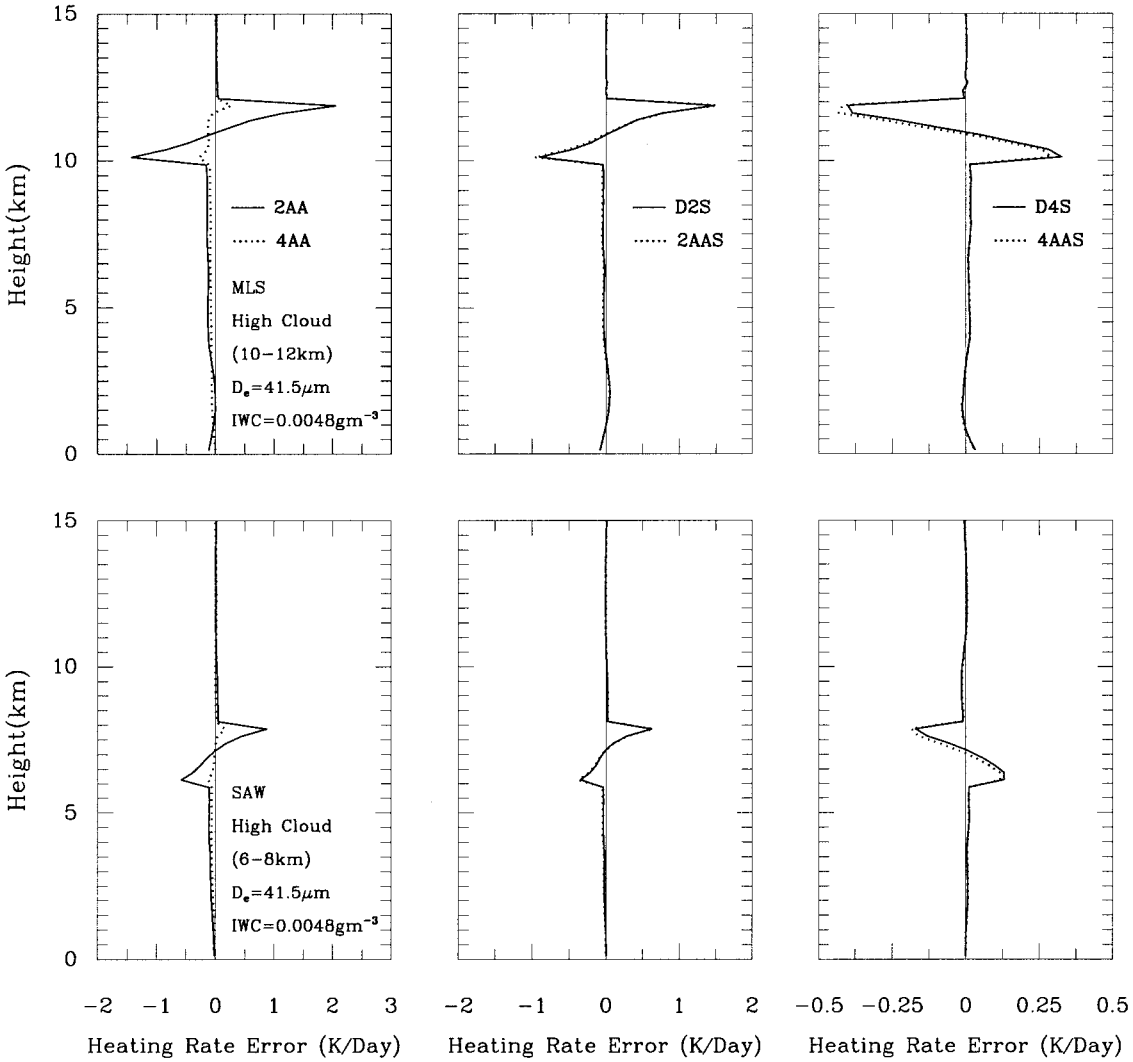

FIG. 3. As in Fig. 1 except for the sky containing the high cloud (in position from 10 to 12 km in MLS and from 6 to 8 km in SAW).

cloud, and the combination of the three clouds. The optical properties of the cloud cases are the same as those in Figs. 1–4.

For a low vertical resolution, the cloud-top cooling cannot be well represented. The large cooling rate at the cloud top is averaged out with the rest of the cloud. Therefore, the cloud cooling rate and the error in cooling rate are all reduced. In other words, the large error in the cloud top is spread out to the whole cloud layer. However, it is found that the situation for errors (not presented) is very similar to that for high vertical resolution. Also, Table 4 shows that the errors in flux are similar to those in high vertical resolution cases.

Both 2AAS and 4AAS are very accurate in comparison with D2S and D4S, respectively. The computational efficiency is another important factor to consider when using absorption approximation with scattering. Figure 5 shows the ratio of timing for 2AAS, 4AA, and 4AAS to 2AA. Only the radiative transfer module is considered, since the time consumed for the rest of the model is the same. For the clear sky, 2AAS costs about 15% more CPU time compared to that of 2AA, 4AA costs about 40% more, and 4AAS costs about 50% more. For 2AAS and 4AAS, the increase in timing is proportional to the number of cloud layers in the column model. The slope of the curve for 4AAS is larger than that for 2AAS, which means that the timing increase with the increase of cloud layers is larger for 4AAS as compared with that of 2AAS. With 20 cloud layers out of a total number of 100 atmospheric layers, the timing ratio is 1.53 for 2AAS and 2.28 for 4AAS. Both are much more efficient than D2S and D4S. According to Fu et al. (1997), the timing ratio is 4 for D2S and 36 for D4S. One reason for dramatically saving computational time for 2AAS and 4AAS is that the cloud-free layers are calculated using the absorption approximation. We would like to point out that in GCMs, the cloud coverage is about 60%, and even for a cloud-covered

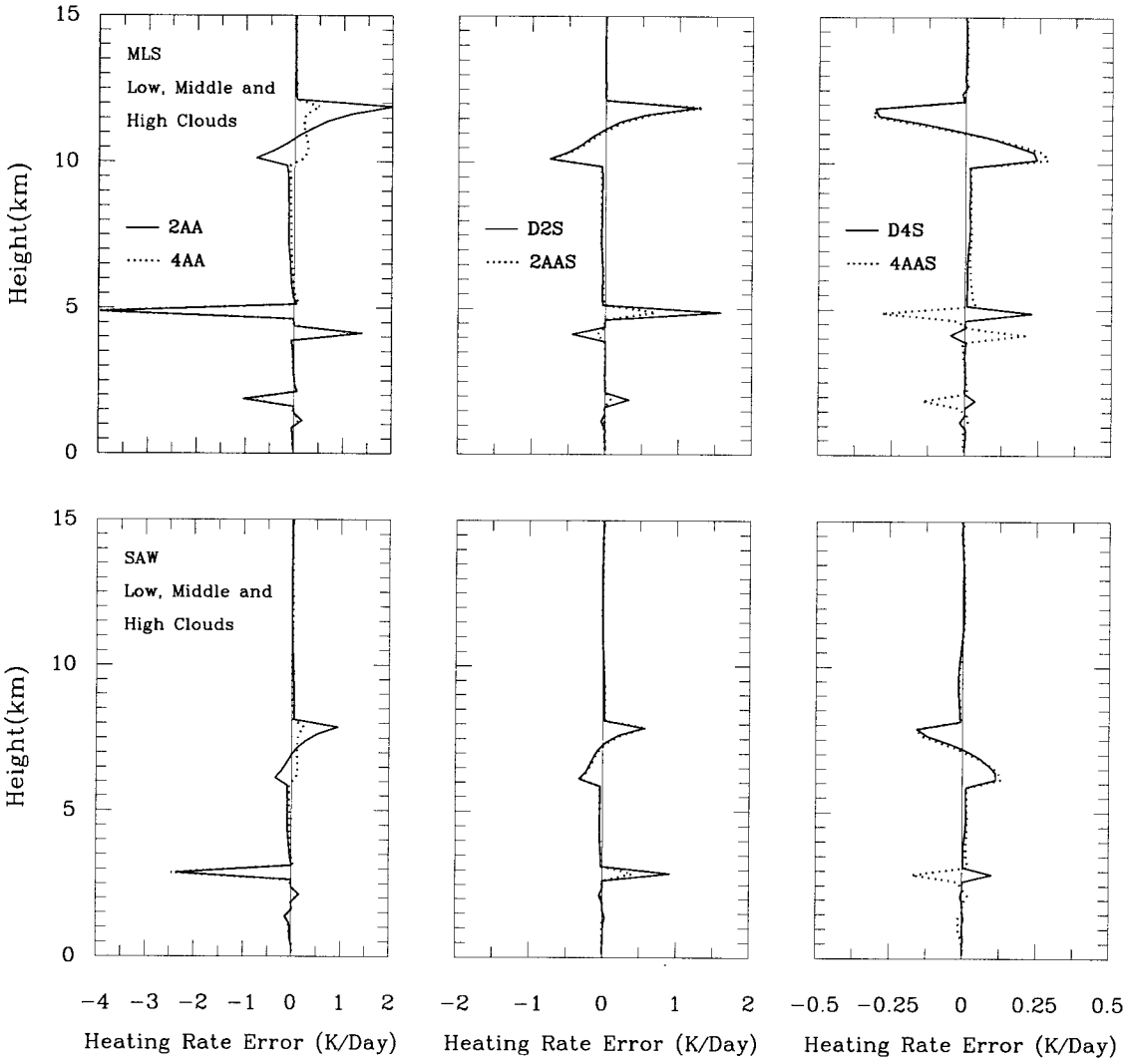

FIG. 4. As in Fig. 1 except for the sky containing the low, middle, and high clouds.

TABLE 4. Same as in Table 2 except with vertical resolution of layer thickness 1 km.

Cloud conditions	D128S	2AA	2AAS	D2S	4AA	4AAS	D4S
				$F^{\uparrow}$ (TOA)			
Low cloud	265.2	270.0 (4.8)	264.5 (−0.7)	262.9 (−2.3)	269.6 (4.4)	265.8 (0.6)	264.6 (−0.6)
Middle cloud	229.2	235.3 (6.1)	228.6 (−0.6)	227.0 (−2.2)	234.9 (5.7)	229.9 (0.7)	228.7 (−0.5)
High cloud	215.0	221.0 (6.0)	214.5 (−0.5)	213.2 (−1.8)	221.4 (5.4)	214.5 (−0.5)	214.1 (−0.9)
Low, middle, and high clouds	187.9	195.9 (8.0)	187.4 (−0.5)	185.8 (−2.1)	195.6 (7.7)	188.1 (0.2)	187.1 (−0.8)
				$F^{\downarrow}$ (SFC)			
Low cloud	411.8	411.2 (−0.6)	411.7 (−0.1)	411.9 (0.1)	411.2 (−0.6)	411.6 (−0.2)	411.7 (−0.1)
Middle cloud	393.4	392.1 (−1.3)	393.5 (0.1)	394.0 (0.6)	392.4 (−1.0)	393.3 (−0.1)	393.6 (0.2)
High cloud	355.6	355.8 (0.2)	356.7 (1.1)	357.1 (1.5)	355.4 (−0.2)	356.1 (0.5)	356.1 (0.5)
Low, middle, and high clouds	411.8	411.2 (−0.6)	411.7(−0.1)	411.9 (0.1)	411.2 (−0.6)	411.6 (−0.2)	411.7 (−0.1)

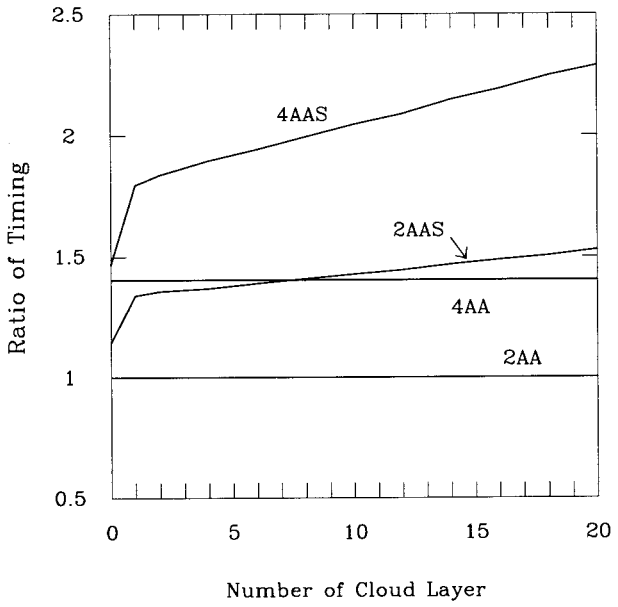

FIG. 5. The timing ratio of 2AAS, 4AA, and 4AAS to 2AA for different cloud layers.

region, most of the model layers are cloud free. Note that 2*n*AAS successfully avoids any scattering calculation in cloud-free layers. So these 2*n*AAS will be very efficient for GCMs.

4. Conclusions

In this work, we have proposed a scheme to deal with scattering in infrared radiation by clouds. This scheme is a perturbation method based on the absorption approximation. The main physical consideration for the scheme is to keep the efficient absorption approximation for cloud-free layers. Different from the source function technology, the lower-order calculation of intensity for the scattering source is based on the absorption approximation instead of the two-stream discrete ordinate approximation. Therefore, this method is much faster than the source function technique. Calculations show that 2AAS is more accurate in heating rate and flux compared with D2S for all the cloud cases considered. The results of 2AAS is very reliable for low and middle clouds. The error in flux at the top of the atmosphere is less 1 W m^{-2}, and the error in heating rate is less than 0.5 K day^{-1}. For high clouds, both D2S and 2AAS do not provide satisfying results. Cloud-top cooling and cloud-bottom warming are always over estimated. It is known from the comparison of 2AA and 4AA that the error in heating rate for high clouds is mostly due to the highly anisotropic distribution of the intensity rather than neglect of scattering. Therefore, a higher-order stream scheme has to be used. The perturbation method proposed in this work is a general method suitable for any stream. It is shown that 4AAS can produce results similar to D4S for low clouds and high clouds. Therefore, 4AAS is a promising method for dealing with scattered infrared radiation.

The program for absorption approximation with scattering effect for infrared radiation is available from the authors.

Acknowledgments. The authors would thank two anonymous reviewers, Drs. H. Barker and M. Holtzer, and Mr. T. H. Lindner for their helpful comments, and Ms. M. C. Cribb for help in running the 128-stream discrete ordinate model. One of authors (QF) has been supported by DOE Grant, NSERC Operating Grant, and AES Science Subvention Grant.

REFERENCES

Edwards, J. M., and A. Slingo, 1996: Studies with a flexible new radiation code. I: Choosing a configuration for a large-scale model. *Quart. J. Roy. Meteor. Soc.,* **122,** 689–719.

Fu, Q., and K. N. Liou, 1992: On the correlated *k*-distribution method for radiative transfer in nonhomogeneous atmospheres. *J. Atmos. Sci.,* **49,** 2139–2156.

——, and ——, 1993: Parameterization of radiative processes of cirrus clouds. *J. Atmos. Sci.,* **50,** 2008–2025.

——, ——, M. C. Cribb, T. P. Charlock, and A. Grossman, 1997: On multiple scattering in thermal infrared radiative transfer. *J. Atmos. Sci.,* **54,** 2799–2812.

Joseph, J. H., W. J. Wiscombe, and J. A. Weinman, 1976: The delta-Eddington approximation for radiative flux transfer. *J. Atmos. Sci.,* **33,** 2452–2459.

Li, J., 1999: Gaussian quadrature and its application to infrared radiation. *J. Atmos. Sci.,* **57,** 753–765.

——, D. J., W. Geldart, and P. Chýlek, 1994: Perturbation solution for 3D radiative transfer in a horizontally periodic inhomogeneous cloud field. *J. Atmos. Sci.,* **51,** 2110–2122.

——, ——, and ——, 1995: Second order perturbation solution for radiative transfer in clouds with a horizontally arbitrary periodic inhomogeneity. *J. Quant. Spectrosc. Radiat. Transfer,* **53,** 445–456.

Stamnes, K., S. C. Tsay, W. Wiscombe, and K. Jayaweera, 1988: A numerically stable algorithm for discrete-ordinate-method radiative transfer in multiple scattering and emitting layered media. *Appl. Opt.,* **27,** 2502–2509.

Toon, O. B., C. P. McKay, and T. P. Ackerman, 1989: Rapid calculation of radiative heating rates and photodissociation rates in inhomogeneous multiple scattering atmospheres. *J. Geophys. Res.,* **94,** 16 287–16 301.